The influence of the milling liquid on the properties of barium titanate powders and ceramics

Hans-Peter Abicht,*[a] Dieter Völtzke,[a] Andreas Röder,[b] Reinhard Schneider[c] and Jörg Woltersdorf[c]

[a]*Fachbereich Chemie, Martin-Luther-Universität Halle-Wittenberg, D-06120 Halle/S, Germany*
[b]*Fachbereich Physik, Martin-Luther-Universität Halle-Wittenberg, D-06120 Halle/S, Germany*
[c]*Max-Planck-Institut für Mikrostrukturphysik, Martin-Luther-Universität Halle-Wittenberg, D-06120 Halle/S, Germany*

The influence of the milling liquid on the properties of donor-doped (La^{3+}) semiconducting barium titanate ($BaTiO_3$) ceramics, generated by the mixed oxide technique, was investigated. Distilled water and propan-2-ol were used as milling liquids. Water was found to have two essential effects. First, it dissolves Ba^{2+} ions out of $BaTiO_3$ grains, thus creating core–shell structures which were confirmed by high-resolution electron microscopy (HREM) and electron energy loss spectroscopy (EELS). They consist of a 3–5 nm thick TiO_x-rich layer followed by a layer (*ca.* 10 nm thick) with a molar Ba/Ti ratio increasing from 0 to 1. These core–shell structures of the $BaTiO_3$ powder positively affect the sintering behaviour of the greens by the high reactivity of the Ti-rich interlayer. Secondly, water cleans the $BaTiO_3$ powder of acceptor contaminants, producing ceramics with a low electrical resistivity at room temperature. Propan-2-ol-milled ceramics of a comparable composition show an electrical resistivity up to six orders of magnitude higher, owing to the compensation of La^{3+}-doping by acceptor contaminants.

Barium titanate ($BaTiO_3$) based ceramics represent an important area within the growing market of functional ceramics. This is true for undoped $BaTiO_3$ ceramics used as dielectrics as well as for doped $BaTiO_3$ used as PTCR (positive temperature coefficient of resistivity) materials.

In recent years, for highly pure $BaTiO_3$ a variety of chemical synthesis methods have been developed (oxalate precipitation, sol–gel procedures, hydrothermal syntheses), but because of high costs they are used for specific applications only. Therefore, the conventional ceramic preparation method (mixed oxide technique, see ref. 1) is still the method of choice. This method includes two milling–mixing steps.

The influence of the milling liquid on the properties of the final ceramics using identical methods and starting materials has not been investigated in detail. Most of the papers presuppose that the stoichiometry, *i.e.* the Ba/Ti molar ratio, is determined by quantity of the starting materials used. Distilled water is the commonly used milling medium. The leaching behaviour during the milling–mixing step has been investigated by Adair *et al.*[2] They reported the dissolution of Ba^{2+} ions from undoped, slightly TiO_2-rich $BaTiO_3$ powders as a function of the pH of the aqueous milling liquid. The microstructure of the leached powders was not studied. The amount of Ba^{2+} leaching was found to affect the amount of exaggerated grain growth during sintering. Adair *et al.*[3] also analysed a large number of organic solvents (with different relative permittivities and electron-donating abilities) with respect to their ability to dissolve Ba^{2+} ions from $BaTiO_3$ particles. No direct comparison between water- and organic solvent-milled $BaTiO_3$ powders was carried out. Investigations concerning the solubility of Ba salts in ethanol, propan-2-ol and alcohol–water mixtures[4,5] proved that they have low solubility in pure organic solvents.

Heywang and Bauer[6] studied wet- and dry-milled Sb_2O_3-doped $BaTiO_6$ powders, revealing essential differences in the electrical properties of the final ceramics. The ceramics of the dry-milled batch exhibited properties of a second-order PTCR element, such as the high electrical resistivity at room temperature, which was attributed to the formation of $Ba(Ti_{0.965}Sb_{0.035})O_3$ shells.

The aim of this study was to analyse the microstructure and microchemistry of the water-leached powders in detail, and to explain the leaching mechanism. Furthermore, the differences in the sintering behaviour and the electrical resistivity at room temperature of the ceramics prepared using either water or propan-2-ol-milled powders are reported.

Experimental

$BaCO_3$ (Merck 1711), TiO_2 (Merck 808) and $La_2(C_2O_4)_3 \cdot 9H_2O$ (SKW Stickstoffwerke Piesteritz) were used as starting materials, and distilled water and propan-2-ol (Merck 109634) as milling media. In a PVC container, the batches were milled for 24 h using PTFE-coated steel balls. The mass ratio $m_{powder} : m_{balls} : m_{liquid}$ was 1 : 1 : 4. After filtering and drying the mixture was calcined in air at 1100 °C for 4 h before it was fine-milled under the same conditions as mentioned above.

The Ba contents of the aqueous milling liquid were analysed gravimetrically as $BaSO_4$. Trace elements and the Ba content in propan-2-ol were determined by atomic absorption spectroscopy (AAS) using a Varian Spectra 20 instrument. The analyses were carried out after both the milling steps.

After fine-milling, filtering and drying the powder was mixed with 5 mass% polyvinyl alcohol solution as a pressing aid. After 24 h it was pressed into pellets (10 mm in diameter and *ca.* 2 mm thick) with a density of 3.1 g cm^{-3}. The greens were sintered at three different temperatures (T_s = 1300, 1350, 1400 °C, dwelling time 1 h).

For testing the electrical resistivity at room temperature the sintered pellets were first polished to flatten the surface followed by electroding with gallium–indium eutectic to provide an ohmic contact. The electrical resistivity was determined by measuring the voltage U and the current intensity I at 22 °C, with U = 0.1 V for low-resistivity samples and with U = 10 V for high-resistivity ones.

Dilatometric investigations were carried out using a SETARAM TMA92 dilatometer (1.0 g loading, Al_2O_3 equipment, 10 K min^{-1} heating rate from 20–1400 °C).

For electron microscope investigations the specimens were prepared by dispersing a small amount of the powder in pure alcohol, mixing it in an ultrasonic generator, and pipetting a

drop of this dispersion on a copper mesh covered with a holey Formvar film.

Electron energy loss spectroscopy (EELS) was applied using a parallel-recording spectrometer (PEELS Gatan model 666) attached to a TEM/STEM Philips CM 20 FEG instrument, run at 200 keV (*ca.* 0.8–1.2 eV energy resolution). Either point analyses were made, or a series of EEL spectra along a line were recorded in the STEM mode, with the electron probe (diameter *ca.* 2 nm) digitally scanned by the Gatan Digiscan model 688. For spectrum processing the software package EL/P from Gatan was used. To minimize or even to avoid contamination during small probe analyses, which can lead to a drastic carbon build-up, the specimen was kept at liquid-nitrogen temperature using a cooling holder (Gatan model 636). High-resolution electron microscopy (HREM) was also applied using a CM 20 FEG microscope.

Results

Milling in water

Batch V1, with $0.001La_2(C_2O_4)_3\cdot 9H_2O : 0.998BaCO_3 : 1.00 TiO_2$ as the starting molar composition, was prepared using distilled water as the milling liquid. After the first mixing–milling process a Ba^{2+} content corresponding to 0.05 mol% of the starting $BaCO_3$ was determined in the water. The fine-milling liquid showed a Ba^{2+} content of 1.46 mol% of the Ba in the calcined powder. The liquid showed a pH value of *ca.* 10, which means that after the ceramic preparation procedure the originally stoichiometric starting mixture had a molar Ba/Ti ratio of 0.985. The results of the AAS analysis of the milling liquids of the first milling and of the fine-milling procedures are summarized in Table 1. The Ba contents are in good agreement with those determined gravimetrically. Ti was not detected, nor was any respective trace. The presence of the trace elements Na, K and Al indicated strong leaching by the preceding aqueous milling, which resulted in a cleaning effect. According to the manufacturer's certificate[7] the $BaCO_3$ used had a contamination level of <50 ppm Al, <50 ppm K and <20 ppm Na. These values were experimentally confirmed to be 25 ppm Na and 30 ppm K. The TiO_2 used (4 g TiO_2 + 56 ml distilled water, 2 h planetary ball mill) was found to contain 830 ppm K and 259 ppm Na as dissolvable contaminants.

Time-dependent leaching experiments and a modified batch V1 with an excess of $BaCO_3$ showed that the dissolved Ba content in V1 is not due to unreacted BaO, but to the leaching of the surface of $BaTiO_3$ grains.

The results of dilatometric investigations of the greens of V1 are presented in Fig. 1(*a*). The shrinkage behaviour is characterized by a pre-densification step beginning at 880 °C, a main densification starting at 995 °C and a shrinkage maximum at 1229 °C. The densification is completed at 1318 °C.

After sintering, the ceramics of batch V1 are dark blue–grey bodies which, when sintered at 1300 °C, show a bimodal grain size distribution with ungrown starting powder (*ca.* 1 μm) and grown grains with diameters of 30–100 μm. Fig. 2 shows the microstructure of a ceramic sintered at 1350 °C. The microstructure is fully grown, consisting of 20–80 μm grains. There is a similar microstructure for the sample sintered at 1400 °C.

Table 1 AAS analysis of the milling liquids after the first mixing–milling step and after fine-milling[a]

	Na (ppm)	K (ppm)	Al (ppm)	Ba (ppm)
V1 (1st milling)	15.9	79.6	6.2	51
V1 (fine-milling)	1.6	15.6	8.2	1440
V2 (1st milling)	<0.1	<0.1	<4	<5
V2 (fine-milling)	0.4	0.34	<4	<5

[a]V1-milling in distilled water; V2 = milling in propan-2-ol.

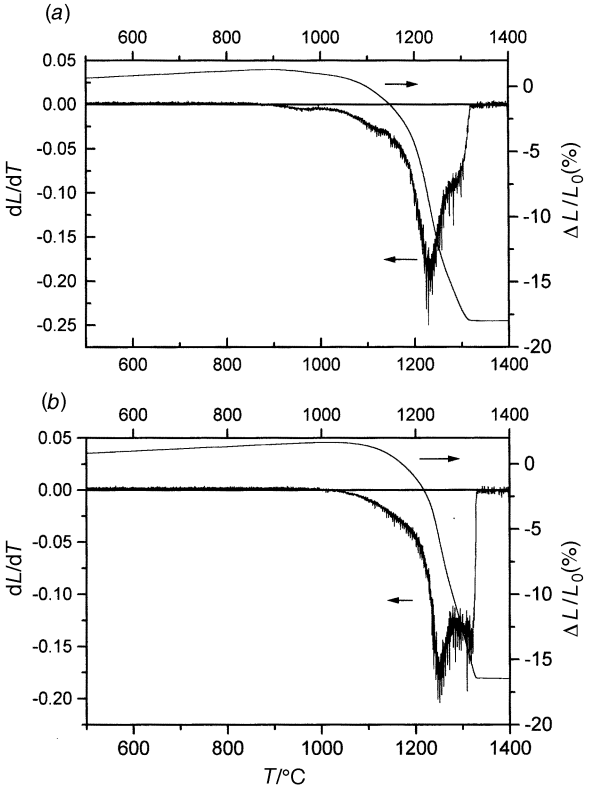

Fig. 1 Shrinkage behaviour of (*a*) greens of batch V1 (starting composition $0.001La_2(C_2O_4)_3\cdot 9H_2O$, $0.998BaCO_3$, $1.00TiO_2$, milled in distilled water), and of (b) greens of batch V2 (starting composition $0.001La_2(C_2O_4)_3\cdot 9H_2O$, $0.998BaCO_3$, $1.02TiO_2$, milled in propan-2-ol).

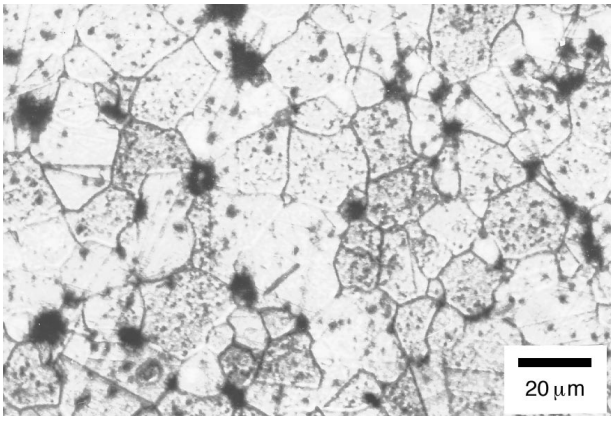

Fig. 2 Microstructure of ceramic V1 sintered at 1350 °C

Milling in propan-2-ol

Ceramics of composition $La_{0.002}Ba_{0.998}Ti_{1+x}O_{3+2x}$ ($x = 0$, 0.005, 0.01, 0.02) were prepared using propan-2-ol as the milling medium to enable with the direct comparison to water-milled samples of similar effective composition. The analysis of the milling liquid of the first and the fine-milling step is exemplary for the propan-2-ol-milled samples V2 given in Table 1. Sample V2 has a composition $La_{0.002}Ba_{0.998}Ti_{1.02}O_{3.04}$. The Ba^{2+} content dissolved in the milling liquid was <0.005 mol%, the trace element concentrations were 3 ppm Na and 2.6 ppm K referring to $BaCO_3$. Al was below the detection limit in the milling liquid.

The dilatometric investigations of the green body V2 are illustrated in Fig. 1(*b*). The shrinkage behaviour is characterized by a beginning of densification at 1020 °C and maxima at 1250 and 1317 °C. The shrinkage is complete at 1338 °C.

Although the effective chemical composition of batches V1

and V2 are nearly the same, there are distinct differences between the two sintered bodies. The colour of the V2 sintered bodies is light-brown, unlike the V1 samples which are blue–grey. The V2 samples, sintered at 1300 °C, show a bimodal grain size distribution of anomalously grown grains and an ungrown matrix [see Fig. 3(*a*)]. The portion of the grown grains in the matrix is smaller than that in V1. The differences between batches V1 and V2 are more pronounced at sintering temperatures of 1350 and 1400 °C. The propan-2-ol-milled samples are not fully grown. There are still areas of fine-grained material (1–2 μm) beside 10–50 μm grains [see Fig. 3(*b*), (*c*)].

Electron probe microanalysis (EPMA; see Fig. 4) revealed that a strongly inhomogeneous element distribution is characteristic of the propan-2-ol-milled batches. The fine-grained areas in the middle of the secondary-electron micrograph of Fig. (4*a*) exhibit a molar Ti/Ba ratio of 0.5 [see line scan in Fig. 4(*b*), (*c*)], corresponding to the composition of barium orthotitanate (Ba_2TiO_4). Ba_2TiO_4 is known to inhibit the grain growth of $BaTiO_3$.[8] On the other hand, only 30 μm from the Ba-rich zone, there is Ti enrichment [at the lower left of Fig. 4(*b*)] with a molar Ti/Ba ratio of 2.0.

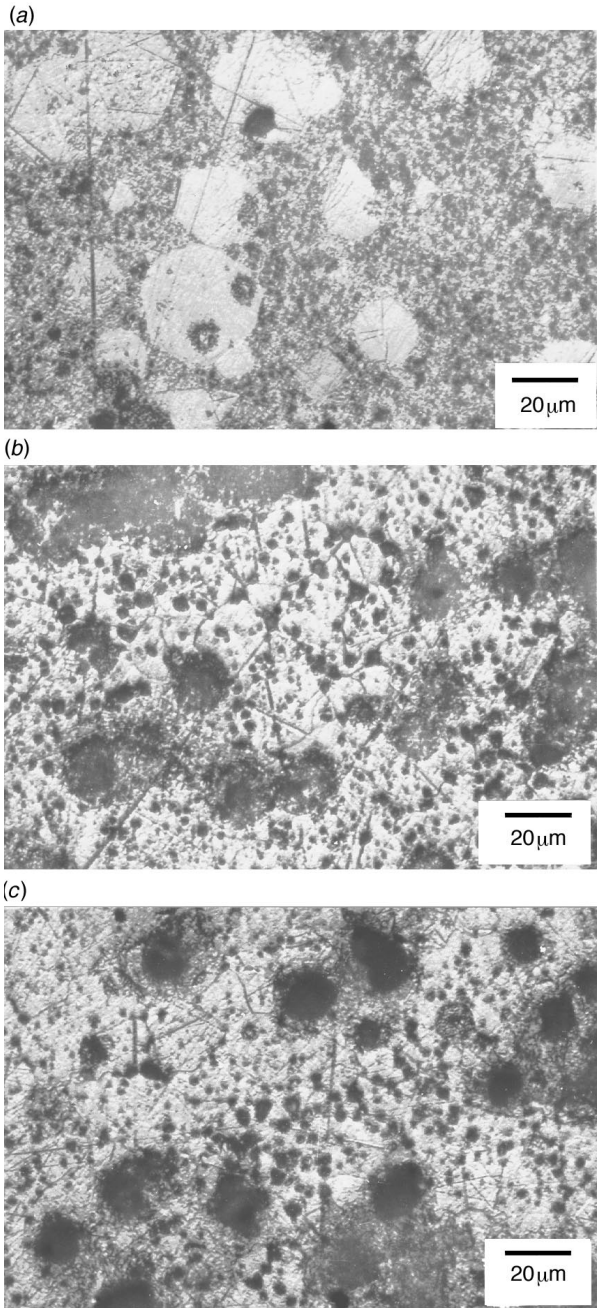

Fig. 3 Microstructure of ceramics V2 sintered at 1300 °C (*a*), 1350 °C (*b*) and 1400 °C (*c*).

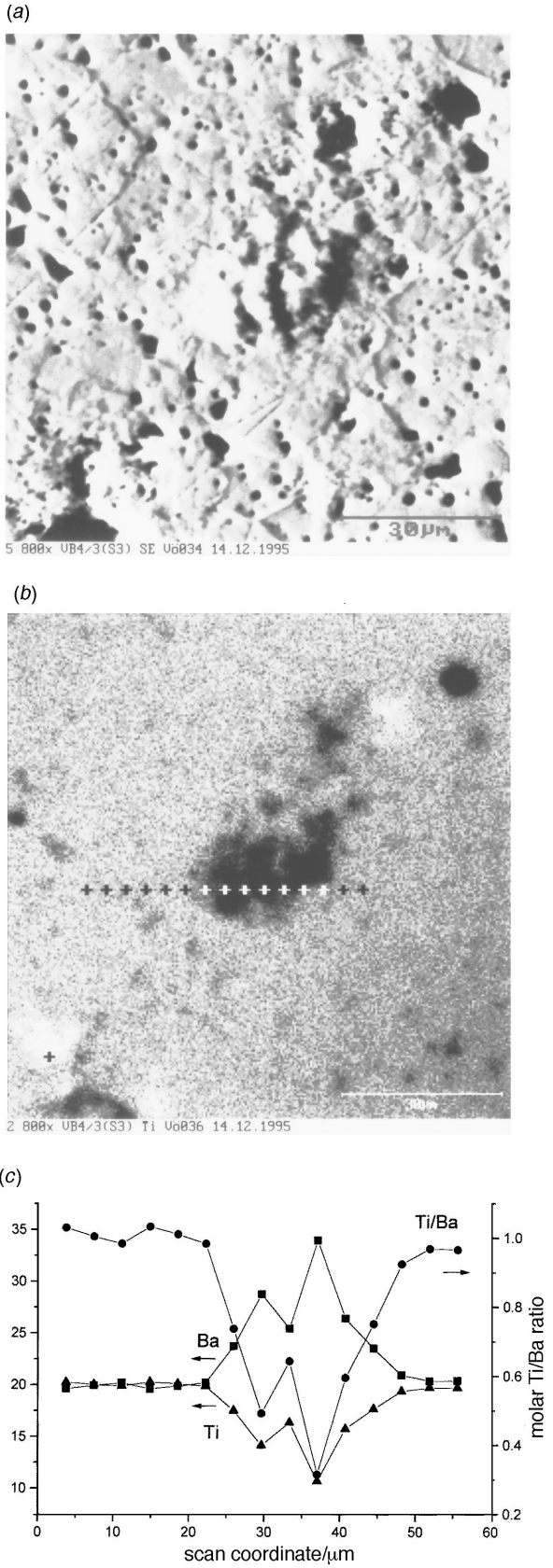

Fig. 4 SE micrograph of sinter V2 (T_s = 1400 °C) (*a*), corresponding Ti mapping (*b*) and element concentrations (*c*) along the line in (*b*).

Discussion

The influence of distilled water as the milling medium on the properties of both the intermediately prepared $BaTiO_3$ powder and the final ceramics can be summarized as follows.

First, during fine-milling Ba^{2+} ions are leached out of the surface of the $BaTiO_3$ grains. This dissolution is facilitated by the mechanical activation of the powder, *i.e.* by the milling balls. It is not prevented by a longer calcination period or higher calcination temperatures.

The dissolution of Ba^{2+} ions from the $BaTiO_3$ structure is supposed to take place according to eqn. (1), using Kröger–Vink notation.

$$(Ba_{Ba} + Ti_{Ti} + 3O_O)_{solid} + 2H_2O \rightarrow$$
$$(Ti_{Ti} + V_{Ba}'' + O_O + 2OH_O^{\circ})_{solid} + (Ba^{2+} + 2OH^-)_{aq} \quad (1)$$

Barium vacancies in the perovskite structure are electrically compensated by hydroxy groups on oxygen sites. The occupation of oxygen sites by hydroxy groups was detected in both single crystals[9,10] and in wet-chemically prepared $BaTiO_3$ powders.[11] In the IR spectra the band (ν_{OH}) of these ions is between 3477 and 3485 cm^{-1}. In the DRIFT spectra of the calcined and fine-milled powder V1 the absorption maximum is at 3609 cm^{-1}. This band lies between the positions of OH groups built into the lattice and surface OH groups (3680–3720 cm^{-1}).[11]

The experimental results can be explained by the formation of core–shell structures consisting of a TiO_2-rich surface layer, followed by a *ca.* 10 nm thick zone depleted in barium (defect perovskite) and a $BaTiO_3$ core. Considering the dissolved Ba content of 1–2 mol% and assuming spherical $BaTiO_3$ grains of 1 μm in diameter a thickness of 1.7–3.3 nm of the Ti-rich shell can be estimated, corresponding to a thickness of 4–8 unit cells of $BaTiO_3$.

The existence of such structures was proved directly by TEM and EELS. However, note that these observations do not apply to all particles in the same way. In particular, it was difficult to find individual particles randomly lying freely over a hole of the supporting film and, in addition, thin enough for EELS analysis (thinner than 50 nm). Part of a typical $BaTiO_3$ particle, tempered at 500 °C, is shown in the HREM image of Fig. 5. The particle is a single crystal, which can be concluded from the atomic rows occurring in its thin regions. However, the particle is partially covered with a thin amorphous layer of *ca.* 3–5 nm thickness. Measurements in the spot mode (electron probe of *ca.* 2 nm in diameter) showed a particular beam sensitivity of this layer, which resulted in damage of the layer after a certain time of illumination. Thus, the conditions for EELS analyses had to be chosen carefully so that information on its composition was not lost. At the same time, on the other hand, owing to the very small thickness of the amorphous layer the degree of inelastic scattering is strongly reduced relative to the inner particle regions, and hence the recording time had to be fitted appropriately to produce a useful signal.

Fig. 5 HREM image of a single $BaTiO_3$ particle partially exhibiting an amorphous surface layer of *ca.* 3–5 nm in thickness

A series of EEL spectra recorded along a line of *ca.* 20 nm length perpendicular to the particle surface (*cf.* marked line in Fig. 5) revealed the element composition of the $BaTiO_3$ particle shown in Fig. 6(*a*). Each spectrum was taken in the energy loss range *ca.* 400–900 eV at an integration time of 4 s with four read-outs accumulated. In Fig. 6(*a*), the lower curves with no notable signal are from the amorphous surface layer. They are followed by spectra with marked Ti L_{23}, O K and Ba M_{45} edges. Appropriate selection of the vertical scale shows that spectra 1 to *ca.* 4, representing the surface layer, primarily exhibit titanium and oxygen with traces of barium [*cf.* Fig. 6(*b*)]. Thus, it can be concluded that this layer is mainly composed of TiO_x. As the spectra are extremely noisy, near-edge structures cannot be resolved, thus no information about the chemical bond state can be deduced.

The remaining spectra (lines 5, 6, 7 *etc.*) show Ti L_{23} edges which, relative to the Ba M_{45} edges, have higher jump ratios (edge maximum-to-background signal) than those in the inner regions of the particle [see upper curves in Fig. 6(*a*)]. This suggests titanium enrichment in the outer periphery of the particle extending from the thin TiO_x-rich surface layer to *ca.* 10 nm into the inner regions, which was proved by quantification. The element concentrations along the line profile of Fig. 6 are given in the plot of Fig. 7. Both the TiO_x -rich layer and the adjoining zone depleted in barium are clearly visible in this diagram. The average composition of the Ti-rich zone is 37±4.9 atom% Ti, 45±6 atom% O and 18±2.4 atom% Ba, whereas in the inner regions of the particle the chemical

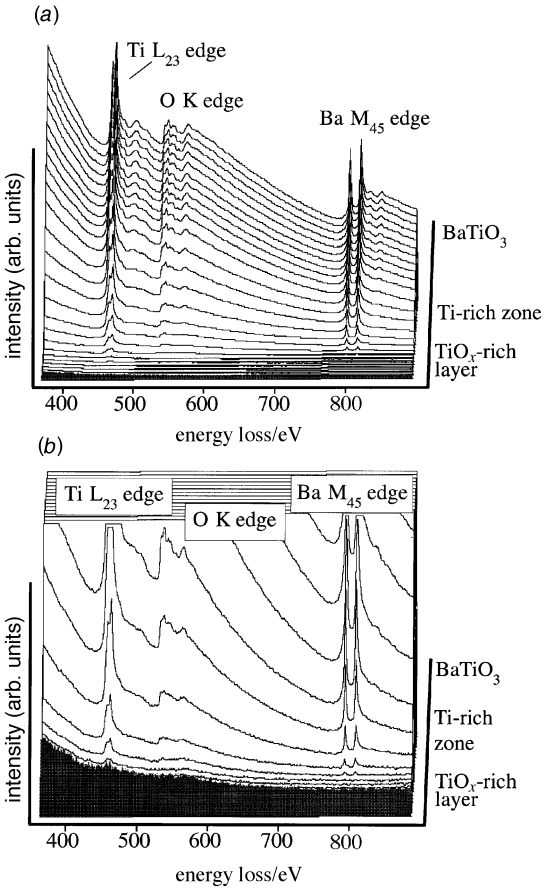

Fig. 6 Element composition of the $BaTiO_3$ particle, shown in Fig. 5, along a line in perpendicular arrangement to the surface, series of EEL spectra (*a*); detailed drawing of those spectra taken from the outermost zone (*b*)

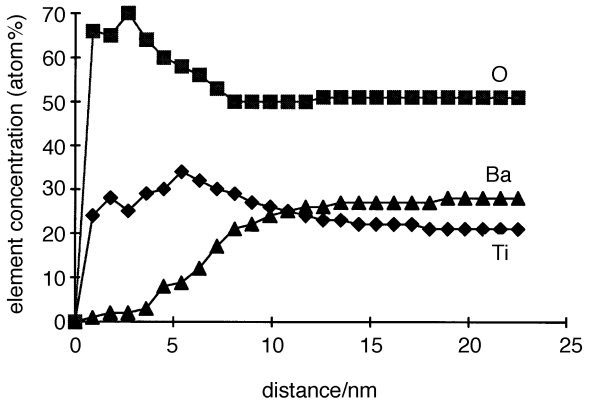

Fig. 7 Element concentrations taken from the line profile of Fig. 6

composition is 23 ± 3.0 atom% Ti, 57 ± 7.6 atom% O and 20 ± 2.6 atom% Ba, which is in good agreement with the stoichiometry of $BaTiO_3$.

Takeuchi *et al.*[12] investigated the phase content of $BaTiO_3$ powders prepared conventionally, and showed that a layer of cubic $BaTiO_3$ had formed at the surface of the grains. The thickness of this surface layer was estimated to be *ca.* 5 nm, irrespective of the grain size of the $BaTiO_3$ powder. If we consider vacancies (V_{Ba}'', $V_O^{\circ\circ}$) producing microstress to be responsible for the stabilization of the cubic phase at room temperature[13,14] the leaching behaviour is easy to explain. The cubic $BaTiO_3$ structure on the surface of the grains, already disturbed by vacancies, is mechanically activated by milling in water. The dissolution of Ba^{2+} ions, creating further V_{Ba}'' sites in the cubic layer [eqn. (1)], results in the formation of a distinctive defect structure.

This surface layer of the grains of batch V1, rich in TiO_2 and defects, is also the reason for the better shrinkage behaviour of the green bodies. Densification processes are causally connected with material transport. If there is no liquid, as occurs with the $BaTiO_3$ system at temperatures below 1320 °C, transport processes occur by solid-state diffusion (grain boundary diffusion). Diffusion processes are essentially influenced by the defect chemistry. The localization of the defects at the surface of the grains is advantageous as the surface diffusion is the mechanism dominant at the initial stage of sintering.[15] According to Valdivieso *et al.*,[16] the presence of hydroxy groups at the surface of $BaTiO_3$ grains has a positive effect on the diffusion and shrinkage processes at 850 °C.

At higher temperatures (>1320 °C), there are optimum conditions for the formation of $Ba_6Ti_{17}O_{40}$ on the TiO_2-rich surfaces of the $BaTiO_3$ grains, and therefore for the formation of $Ba_6Ti_{17}O_{40}$–$BaTiO_3$ eutectic, and consequently for liquid-phase sintering. The result is a fully grown microstructure of the sinters.

The resulting excess of TiO_2 (batch V1) is distributed homogeneously over the surface of the grains, whereas in case of batch V2 (propan-2-ol milled) the excess TiO_2 initially added is distributed randomly in the mixture, resulting in locally different Ba/Ti ratios and an inhomogeneous microstructure after sintering.

Secondly, water as the milling liquid purifies the starting materials ($BaCO_3$, TiO_2) and the $BaTiO_3$ powder from acceptor impurities. Chemical analyses reveal the contents of dissolved impurities to be 0.0845 mol% Na, 0.264 mol% K and 0.054 mol% Al (in total 0.4025 mol% of impurities). These ions act as acceptors, having a counteracting effect on the semiconductivity of La^{3+}-doped $BaTiO_3$. These impurity contents remain within the propan-2-ol-milled batch V2 so that the effect of La^{3+}-doping should be eliminated.

In Table 2 the electrical resistivities of ceramics V1 and V2 at room temperature are summarized. Comparison of the values of the electrical resistivity shows clearly the differences between water-milled and propan-2-ol-milled ceramics with a comparable composition of $La_{0.002}Ba_{0.998}Ti_{1.02}O_{3.04}$. For the propan-2-ol-milled ceramics (despite the remarkable grain growth implying grains of diameter 20–50 μm), the electrical resistivity of up to six orders of magnitude higher results from the compensation of the La^{3+}-doping by acceptor contaminants.

Table 2 Electrical resistivity at room temperature of La^{3+}-doped $BaTiO_3$ ceramics prepared with distilled water (V1) and propan-2-ol (V2) as milling media

sintering temperature/°C	ρ/Ω cm	
	V1	V2
1300	41.7	35.5×10^6
1350	7.7	39.0×10^6
1400	9.2	8.3×10^6

This is our explanation for the differences in the electrical properties of wet and dry-milled batches described by Heywang and Bauer.[4]

Summary

Two ceramic batches were prepared using the same starting materials and the same technology but different milling media (distilled water, propan-2-ol). The final ceramics showed distinct differences in their microstructure and electrical properties. The differences are attributed to the interaction of water with the starting materials and the calcined powder. The interaction takes place in two ways:

(1) Water dissolves Ba^{2+} ions out of the $BaTiO_3$ grains thus creating core–shell structures, which were proved directly by HREM and EELS. Next to a 3–4 nm thick TiO_x-rich surface region a *ca.* 10 nm thick defect perovskite structure is detected, in which Ba vacancies are electrically compensated by hydroxy groups at oxygen sites. The molar Ba/Ti ratio increases from 0 to 1. These core–shell structures are typical of the water-milled $BaTiO_3$ grains and positively affect the sintering behaviour.

(2) Water has a purifying effect on the acceptor contaminants of the starting materials. If not eliminated, these contaminants will counteract the semiconductivity arising from donor doping, thus causing high electrical resistivity.

The authors gratefully acknowledge the financial support of this work by the Deutsche Forschungsgemeinschaft and the Fonds der Chemischen Industrie.

References

1 A. Bauer, D. Bühling, H-J. Gesemann, G. Helke and W. Schreckenbach, in *Technologie und Anwendungen von Ferroelektrika*, Akademische Verlagsgesellschaft Geest & Portig K.-G., Leipzig, 1976, pp. 199 ff.
2 D. A. Anderson, J. H. Adair, D. V. Miller, J. V. Biggers and T. R. Shrout, *Ceram. Trans.*, 1988, **485**, 485.
3 D. V. Miller, J. H. Adair and R. E. Newnham, *Ceram. Trans.*, 1988, **485**, 493.
4 W. Heywang and H. Bauer, *Solid State Electronics*, 1965, **8**, 129.
5 G. W. Ferner and M. G. Mellon, *Ind. Eng. Chem.*, 1943, **6**, 345.
6 Landolt-Börnstein, *Gleichgewichte-Lösungsgleichgewichte*, Springer-Verlag, Berlin, 1962–1964, vol. 2, part 2b, pp. 3–618 ff.
7 E. Merck, Dept. SFC/V, Tl, Data sheet Barium carbonate Selectipur, 1711.
8 R. K. Sharma, N. H. Chan and D. M. Smyth, *J. Am. Ceram. Soc.*, 1985, **68**, 372.

9 A. Jovanovic, M. Wöhlecke, S. Kapphan, A. Maillard and G. Godefroy, *J. Phys. Chem. Solids*, 1989, **50**, 623.
10 R. Waser, *Ber. Bunsen-Ges. Phys. Chem*., 1986, **90**, 1223.
11 G. Busca, V. Buscaglia, M. Leoni and P. Nanni, *Chem. Mater*., 1994, **6**, 955.
12 T. Takeuchi, K. Ado, H. Kagegawa, Y. Saito, C. Masquelier and O. Nakamura, *J. Am. Ceram. Soc*., 1994, **77**, 1665.
13 D. Völtzke and H-P. Abicht, *J. Mater. Sci*., 1995, **30**, 4896.
14 J. M. Criado, M. J. Dianez, F. Gotor, C. Real, M. Mundi and S. Ramos, *Ferroelectr., Lett. Sect*., 1992, **14**, 79.
15 J-L. Hebrard, P. Nortier, M. Pijolat and M. Soustelle, *J. Am. Ceram. Soc*., 1990, **73**, 79.
16 F. Valdivieso, M. Pijolat, C. Magnier and M. Soustelle, *Solid State Ionics*, 1996, **83**, 283.

Paper 6/04730K; *Received* 5*th July*, 1996